PHYSICAL REVIEW B VOLUME 19, NUMBER 12 15 JUNE 1979

Dielectric constant of gold, copper, and gold-copper alloys between 18 and 35 eV

D. Beaglehole* and M. De Crescenzi†
Groupe de Physique des Etats Condensés, Marseille-Luminy, France

M. L. Thèye and G. Vuye
Laboratoire d'Optique des Solides, Université P. et M. Curie, Paris, France
and Laboratoire d'Utilisation du Rayonnement Electromagnétique, Bâtiment 209C, Université de Paris-Sud, Orsay, France
(Received 24 October 1978)

The complex dielectric constant of Au, Cu, and Au-Cu alloys has been determined between 18 and 35 eV from multiangle reflection measurements performed with the ACO synchrotron radiation source. The different techniques as well as the reliability and accuracy of the results are discussed in detail. The optical properties of pure Au and pure Cu are compared, and their modifications upon alloying are investigated by both static and differential experiments. Special attention is paid to pure Au, where fine structure in the main absorption peak is related to the presence of two critical points, the location of which is discussed. The Au spectrum is found to be rather insensitive to alloying with Cu, while on the Cu-rich side the behavior is completely different; different interpretations are proposed.

I. INTRODUCTION

The optical properties of the noble metals and their alloys have been extensively investigated in the visible and near-ultraviolet range by static and modulation (thermoreflectance, piezoreflectance) techniques and are presently well understood.[1] The electronic band structures a few eV on both sides of the Fermi level have been accurately determined and it has been demonstrated in the case of Cu that theoretical computations are able to reproduce the experimental optical absorption within the one-electron picture, not only in energy position of the different structures, but also in absolute magnitude.[2] On the contrary at higher energies, although the gross features of the optical properties have been established a long time ago with conventional sources,[3-8] little effort has been dedicated to the interpretation of the data. Up to 50 eV, the optical absorption is still dominated by electronic excitations from the filled d bands located a few electron volts below the Fermi level to excited states higher in the conduction band. Attempts at determining the empty part of the electronic band structure at such high energies have already been made, at least for Cu,[9] and for Au,[10,11] but the exact position as well as the identification of the different states are still uncertain.

The recent development of synchrotron radiation sources has made more detailed investigations of these metals and their alloys possible over a wide spectral range in the middle and far ultraviolet, by high-resolution optical or photoemission experiments. Quite recently, the properties of Au in the 6–35-eV range have been considered again, special attention being paid to the region where Au presents a quite strong absorption peak, i.e., 18–25 eV. Thermoreflectance measurements,[12,13] as well as constant initial-state energy photoemission spectroscopy,[14] have revealed new structures in the spectra and emphasized a possible role of $5d$ to $5f$ transitions in this spectral range. However, a reliable assignment of the various structures is still lacking. We have, therefore, undertaken a comparative study of the two noble metals Au and Cu in a spectral range in which both metals present an absorption maximum of unequal strength, i.e., from 18–35 eV. Our purpose was to determine their complex dielectric constant directly in absolute magnitude with high energy resolution, from the analysis of multiangle reflectivity measurements. For these experiments, we have used the synchrotron radiation source ACO of Laboratoire d'Utilisation du Rayonnement Electromagnétique (LURE), Orsay, taking into account the polarization of the incident beam in our experimental situation. Besides the pure metals, we have also investigated the optical properties of their alloys for various concentrations, in order to better understand the nature of final states in both metals through their modification upon alloying. These alloy studies have been performed by the same method as for pure Au and pure Cu, and also by a differential method, which might be applied as well to different problems such as surface layers, etc.

We describe first the principle of the method and give a critical analysis of its possibilities and of the difficulties encountered in our special experimental conditions. We then describe briefly the experiment. The results obtained for the complex dielectric constant of pure Au, pure Cu, and of their alloys as a function of composition are compared and discussed.

II. TECHNIQUE

A. Reflectivity measurements

The reflectivity R of an opaque sample at a given wavelength depends upon the angle of incidence θ and the polarization of the light beam, and upon the complex dielectric constant $\epsilon = \epsilon_1 + i\epsilon_2$ of the material which we want to determine. (We assume that the sample is homogeneous, which is achieved by thorough annealing, and that no surface layers are present.) With special care in the experimental configuration, it is possible with a synchrotron radiation source to achieve a high beam polarization in the vacuum ultraviolet, but commonly such special care has not been taken; this was our situation and it was necessary to treat the polarization as an additional quantity to be fixed by the measurements. The intensity incident onto the sample can be decomposed into components with s and p polarization, I_s and I_p, respectively, perpendicular and parallel to the plane of incidence. Writing $\alpha = I_s/(I_s + I_p)$, we have the experimental reflectivity $R = \alpha R_s + (1-\alpha)R_p$. [The polarization is sometimes characterized by $P = (I_p - I_s)/(I_p + I_s)$, then $P = 1 - 2\alpha$.]

The angular dependent reflectivity $R(\theta)$ is thus a function of three unknowns, $\epsilon_1, \epsilon_2, \alpha$. Measurements of the reflectivity at a minimum of three angles of incidence are necessary to fix these three unknowns. In practice, as we shall see, the presence of experimental errors require that measurements be taken at more than three angles to adequately determine the unknowns. A different way of solving the problem[15,16] consists of taking an average of reflectivities after a rotation of the reflectivity chamber by 90° about the beam direction. This is a useful (though cumbersome) technique since the rotation averages the polarization, and one is then dealing with a well-defined α of 0.5.

In order to determine the best range of θ to use in the experiments for an accurate determination of $\epsilon_1, \epsilon_2, \alpha$, we made model calculations of the rms errors in ϵ_1, ϵ_2, and α, using values of ϵ_1 and ϵ_2 appropriate to the vacuum ultraviolet region and assuming 1% fractional errors in measurements of R at three angles of incidence. The results of these calculations[17] showed that spacing the angles as widely apart as possible increased the sensitivity to both ϵ and α. We have also constructed isoreflectance curves in the (ϵ_1, ϵ_2) plane for several angles of incidence and for $\alpha = 0.0$, 0.5, and 1.0. Figure 1 shows the results for an angle of incidence θ of 30° and for $\alpha = 0.0$ and 1.0, for the range of ϵ_1 between −2 and +3 and of ϵ_2 between 0 and +2. These curves are useful in providing a graphical solution for the three unknowns

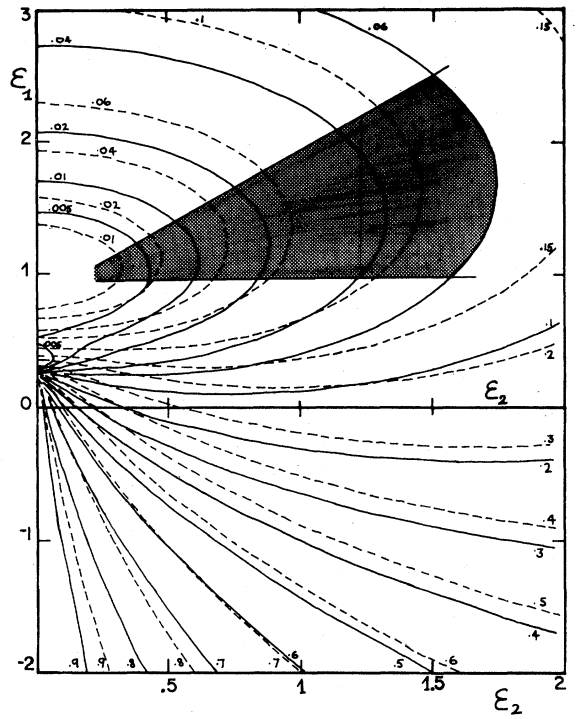

FIG. 1. Isoreflectance curves in the (ϵ_1, ϵ_2) plane for the two extreme values of the polarization α: 0.0 (continuous lines) and 1.0 (dashed lines), and for the angle of incidence $\theta = 30°$. The shaded area indicates the region of sensitivity to ϵ_2.

and in determining uncertainties in the solutions. The isoreflectance curves for other angles of incidence are similar to those for 30° but become increasingly expanded as θ increases.

Some properties of the reflectivity are clear from these curves: (i) at small angles of incidence, the reflectivity is sensitive to values of both ϵ_1 and ϵ_2. The region of predominant sensitivity to ϵ_2, shown in Fig. 1 by the lightly shaded area, is small and essentially independent of α. Thus one must be cautious in associating structure in R directly to structure in ϵ_2; it may just as well arise from changes in ϵ_1, as indeed we find the case for Au; (ii) for a given value of the dielectric constant, the reflectivities are highest for s-polarized light ($\alpha = 1.0$); (iii) the dielectric constant is best defined by measurements with p-polarized light ($\alpha = 0.0$), with an important proviso that since the small-angle reflectivities are very low, the improvement in sensitivity to ϵ may be lost by larger errors in the reflectivity measurement. (It is not easy to reduce the error in an absolute reflectivity measurement below a value of 0.005 since a reflectivity determination requires two measurements, the direct and the re-

flected intensities, for which the light has an inverted distribution across a photodetector that never has uniform spatial sensitivity.)

B. Differential reflectivity measurements

A useful technique for reducing the impact of systematic errors is that of differential reflectivity, where one compares two samples with reflectivities R_1 and R_2 in a periodic fashion and measures the quantity $\beta = 2(R_1 - R_2)/(R_1 + R_2)$ directly. The technique can be applied to the study of surface layers[18,19] or to bulk changes in the sample associated with alloying.[20] It is not a true modulation technique in the sense that the properties of one sample are modulated periodically, but a differential technique in the proper sense of the term. By comparing two samples (which may have quite different properties) at the same time, many of the systematic errors in alignment, in beam intensity, polarization, and distribution, in surface contamination, etc. are reduced.

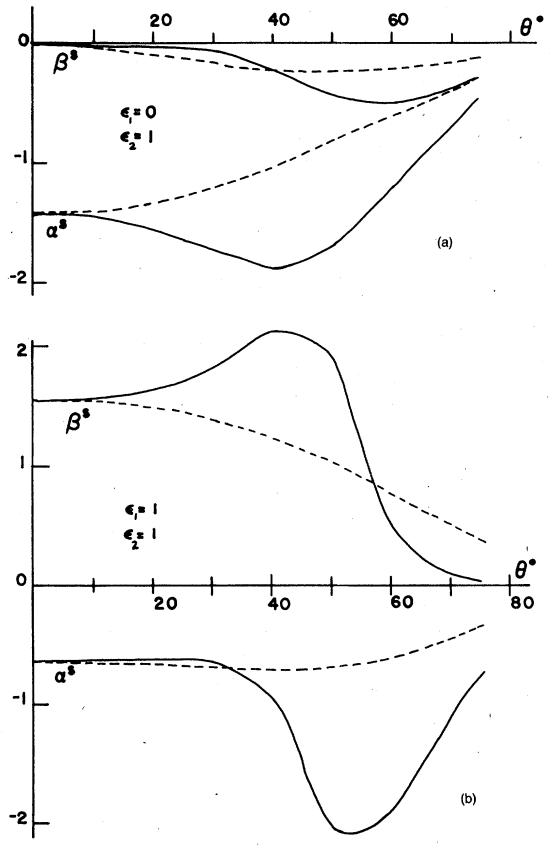

FIG. 2. Variations of the Seraphin coefficients (see text) α^S and β^S with the angle of incidence for s (continuous lines) and p (dashed lines) polarizations, for two sets of values of ϵ_1 and ϵ_2: (a) $\epsilon_1 = 0$, $\epsilon_2 = 1$, and (b) $\epsilon_1 = 1$, $\epsilon_2 = 1$.

The modulation and differential techniques are often applied to the normal-incidence reflectivity only, and one is unable to determine the changes in dielectric constant directly. We have made measurements at several angles of incidence θ and have thus found $\Delta\epsilon_1$ and $\Delta\epsilon_2$ directly, $\Delta\epsilon_1$ and $\Delta\epsilon_2$ being the differences in ϵ_1 and ϵ_2 between the two samples. For small changes in ϵ, one can write the change in reflectivity as $\Delta R/R(\theta) = \alpha^S \Delta\epsilon_1 + \beta^S \Delta\epsilon_2$, where α^S and β^S, the Seraphin coefficients,[21] are functions of ϵ_1 and ϵ_2, θ and α. Figure 2 illustrates the variations of α^S and β^S with angle of incidence for s- and p-polarized light for values of ϵ_1 and ϵ_2 typically found in the vacuum ultraviolet. It can be seen that the coefficients vary most with angle of incidence with p-polarized light, so this would be the preferred polarization for differential measurements.

In our use of this technique we have first measured $R(\theta)$ for one sample to find ϵ_1, ϵ_2, and α, and have then performed the differential measurements. To find $\Delta\epsilon_1$ and $\Delta\epsilon_2$ we have taken α to have the value obtained in the first experiment and, rather than use the first order expression above, we have written $R_2 = R_1(1 - \frac{1}{2}\beta)/(1 + \frac{1}{2}\beta)$ and evaluated the changes in the dielectric constant exactly.

C. Experiment

The optical measurements were performed with the synchrotron radiation from the ACO storage ring (LURE, Orsay) between 16 and 40 eV. The ultrahigh vacuum (ion pump and liquid-He cryopump) experimental chamber contained an evaporation set-up for depositing pure metal or alloy films and a precision goniophotometer for *in situ* reflectivity measurements at different angles of incidence between 30° and 70°. Before entering the experimental chamber, the light was deflected upwards and sidewards with respect to its initial direction by a series of toroidal and plane mirrors and was dispersed horizontally by a normal incidence monochromator. Between the monochromator and the main chamber, the light passed through a first chamber (also serving for differential pumping) containing a toroidal platinum mirror working at 60° angle of incidence, which focused the beam onto the sample. In such an experimental situation, the incident light was likely to have lost much of its initial horizontal linear polarization. Independent measurements of the beam polarization performed at another exit of the same monochromator (one plane mirror less on the light line) in the 17–25-eV range indeed showed that the light was elliptically polarized, the small axis (close to vertical) increasing with

increasing energy around 25 eV, while the ellipse was rotating away from the horizontal.[22] We shall see that qualitatively similar results (taking into account the presence of two more mirrors on the beam in our case) were deduced from our measurements. In addition to this depolarization of the beam, which proved to be rather unfavorable for the sensitivity of the method which we had chosen, the presence of so many mirrors on the light line led to an effective intensity about as large as that of a conventional source, and caused spurious effects on the intensity and polarization of the beam, mainly due to contamination layers on the mirrors. For all these reasons, as emphasized in Sec. II A, we were obliged to take the polarization of the incident light as an unknown, and to determine it from our measurements together with the optical constants. On the other hand, we found that the beam had a short-term stability of 1 in 10^4 (over periods of about 1 sec), superimposed on a long-term drift as the storage-ring current decreased. This encouraged us to develop the differential technique for studying alloying (and surface layer) effects. The samples were opaque (about 1000-Å thick) films of the pure metals Au and Cu and of their alloys with various compositions, deposited by coevaporation with a two-crucible electron gun onto glass substrates polished to a supersmooth finish (7–10-Å rms roughness) and carefully cleaned. The pressure during evaporation rose from the 10^{-8}-Torr to the 10^{-7}-Torr range. The thickness and composition of the deposits were controlled by a quartz microbalance after suitable calibration. The films could be annealed *in situ* just after deposition with a radiating oven. The alloy composition was determined *a posteriori* from the value of the lattice parameter as deduced from x-ray diffraction measurements with 1% accuracy.

The optical measurements were performed *in situ* with the help of the precision goniophotometer located inside the same vacuum chamber. It consists of two concentric rings supporting the sample holder and the light detector, respectively, which are rotated about the same axis (θ-2θ movement). The angular accuracy of the goniometer is 0.01°. The sample holder has two positions: a horizontal one for film deposition and annealing (and possibly surface examination) and measurement of the incident intensity (sample out of the beam), and a vertical one with a precise alignment of the sample surface on the goniometer axis for measurement of the reflected intensities (sample on the beam). Two light detectors were successively used in two different sets of experiments: a channeltron in the 10–40-eV range, then a conventional photomultiplier–sodium-salycilate combination in the 16–35-eV range. The photomultiplier was eventually preferred, because the channeltron proved to be far too position sensitive for such precision measurements at different angles of incidence, even with good optical alignment. An aperture mask was placed in front of the photomultiplier in order to define the detector position; a cooling manifold was used to prevent heating of the photocathode during bakeout.

A Wood's anomaly in the efficiency of the monochromator grating at 357 Å provided both an accurate wavelength calibration and an estimation of second-order light intensity by looking at the corresponding residual second-order peak at 714 Å. In both sets of experiments, results free from second-order effects were obtained for energies greater than 18 eV. On the high-energy side, the photomultiplier was sensitive to stray light and the data above 30 eV were systematically discarded. With the channeltron it was possible to go to higher energies but with less accuracy than below 30 eV due to the rapid decrease of the intensity.

The light detector output was recorded each 1 Å on magnetic tape with the help of the LURE data acquisition facilities. The measurements were made continuously with wavelength and the data thus had the resolution of the monochromator, which was about 1 Å. The data were subsequently punched out on computer cards for analysis.

In addition to these static measurements, we performed, in the same vacuum chamber, the differential measurements based on a tuning-fork technique. The sample holder was simply replaced by a vibrating one, bringing alternatively into the beam the two halves of a substrate with pure metal on one half (reflectivity R_1) and an alloy on the other (reflectivity R_2). The signal, measured by conventional modulation techniques, was $\beta = 2(R_1 - R_2)/(R_1 + R_2)$. These measurements were also made at different angles of incidence. A calibration for β was obtained by deflecting the beam to one edge of the sample, thus putting R_2 equal to zero. The noise in the synchronous signal with a 3-sec time constant and a 1-Å bandwidth corresponded to a value of β of ± 0.002, the signal itself being of the order of 0.1

III. EXPERIMENTAL RESULTS

A. Analysis of the data

The experimental procedure measured first the incident intensity (sample out of the beam), then the reflected intensity at seven angles of incidence: 30°, 40°, 50°, 55°, 60°, 65°, and 70°. The data had to be corrected for: (i) zero (dark) intensity, which could be quite large compared to the signal

when the measurements were made with the photomultiplier, in particular for Cu at high energies, where the reflectivity falls off very rapidly; (ii) decrease with time of the incident intensity, which can be approximated by $e^{-\Gamma t}$; Γ was determined by fitting the results of repeated measurements of $R(70)$ at different times during the experiment by an expression of the above form; Γ was of the order of 0.0035 min^{-1}. The whole set of $R_\theta(\omega)$ curves were then obtained by dividing the corrected reflected intensities by the corrected incident intensity. The $R(\theta)$ data obtained with the photomultiplier were smoothed by various weighted linear interpolation procedures over three or five points (one point each 1 Å).[23] No such treatment was necessary for the data obtained with the channeltron.

The $R_\theta(\omega)$ values obtained with the photomultiplier were estimated to have about 1% absolute fractional error up to 25 eV, a few percent at higher energies. The values obtained with the channeltron suffered from systematic errors due to inaccuracy in alignment. While the absolute values of $R(\theta)$ were in error, the alignment problem would not affect their spectral dependence. We therefore used scaling procedure for this data, bringing the values of $R(\theta)$ at $\hbar\omega = 22$ eV to be identical to the values computed using ϵ_1 and ϵ_2 determined from the photomultiplier data and a mean value for the polarization α. These scaled experimental curves $R_\theta(\omega)$ were then used in the usual fitting procedure to calculate the three parameters ϵ_1, ϵ_2, and α at each energy. Different values of α were chosen for the scaling procedure, the one offering the best self-consistency in the whole process being retained in the end. While we do not place confidence in the absolute values of ϵ_1 and ϵ_2 determined in this way, we have used these results to compute the derivatives $\partial\epsilon_1/\partial\omega$ and $\partial\epsilon_2/\partial\omega$ (as well as $\partial R/\partial\omega$) rather than the photomultiplier results because of their much lower noise.

A least-square fitting program (BMDX-85 from the UCLA computer library[24]) was used to determine the three parameters ϵ_1, ϵ_2, and α from the seven values $R(\theta_i)$ at each wavelength. The residual mean-square deviation per point was usually of the order of 10^{-5} to 5×10^{-5}, rising to a few 10^{-4} at the highest energies, where the experimental uncertainties on R were larger. Figures 3 and 4 show typical results (continuous curves) of the determination of (a) ϵ_1 and ϵ_2 and (b) α as a function of energy in the case of pure Au and pure Cu, respectively. In all experiments, the polarization factor α remained approximately constant at low energies, from 18 up to about 25 eV, then increased steadily towards 1 as the energy

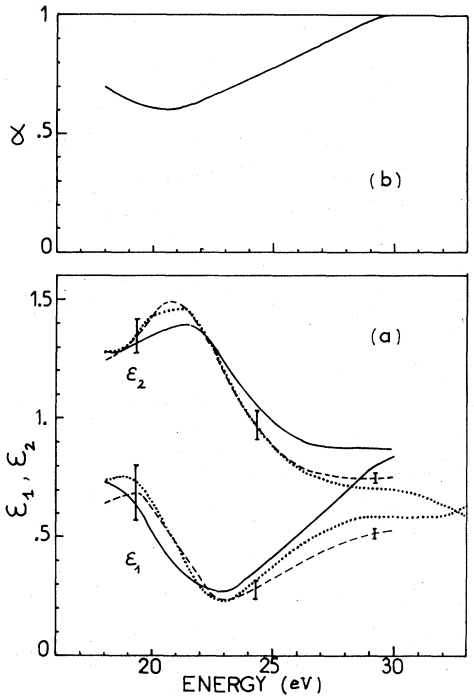

FIG. 3. (a) ϵ_1 and ϵ_2 and (b) α as a function of energy between 18 and 30 eV as determined simultaneously from photomultiplier reflectivity data for pure Au (continuous lines). The ϵ_1 and ϵ_2 spectra obtained by fixing α at 0.65 (dashed lines), as well as those deduced from channeltron data (with $\alpha = 0.50$) (dotted lines) are also indicated. The error bars on the latter curves correspond to the changes in ϵ producted by changes in α of ± 0.05.

increased. The approximately constant value at low energies depended on the experimental conditions (i.e., the characteristics of the incident beam in the particular run) but always lay between 0.5 and 0.8, while the increase at higher energies was more or less rapid. This means that in our experimental situation the incident light was predominantly s polarized in the whole spectral range (in spite of the initial p-polarization of the source) and that its state of polarization varied with energy as well as from one run to another.

Usually α reached 1 at 30 eV. We have already emphasized that our experimental data suffered from stray light effects above 30 eV and became less accurate, which is presumably the reason for the unphysical result of α greater than 1. However, we take the increase of α from 25–30 eV as real in agreement with the conclusion of the direct determination of the beam polarization mentioned above.[22]

When using such a fitting procedure with three parameters, one must take into account the fact that the parameters are strongly correlated. The

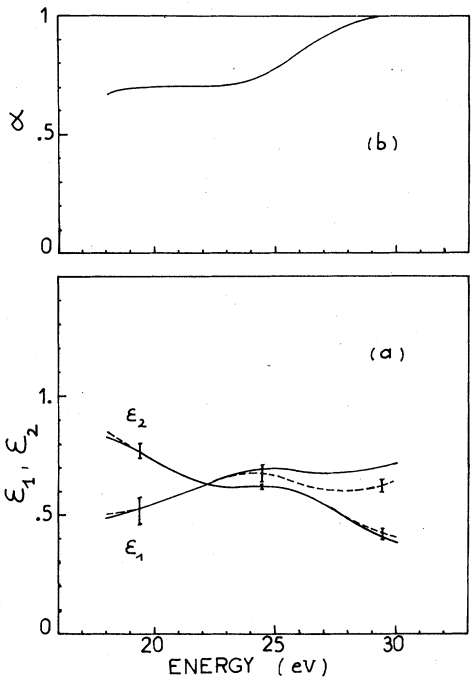

FIG. 4. (a) ϵ_1 and ϵ_2 and (b) α as a function of energy between 18 and 30 eV as determined simultaneously from photomultiplier reflectivity data for pure Cu (continuous lines). The ϵ_1 and ϵ_2 spectra obtained by fixing α at 0.70 (dashed lines) are also indicated. The error bars on the latter curves correspond to the changes in ϵ produced by changes in α of ± 0.1.

program gives the correlation coefficient matrix, which showed a very strong correlation between ϵ_1 and α, and a still important correlation between ϵ_2 and α. If now α was considered as known and fixed to a certain value (depending or not on energy), the fitting procedure with only two parameters ϵ_1 and ϵ_2 gave very reliable results. In a second step, we have therefore given to α, either the values deduced by smoothing the $\alpha(\omega)$ curves obtained above, or a constant value equal to the mean value in the low-energy range, and we have computed ϵ_1 and ϵ_2 again. This procedure provided a check on the results of the first step and also allowed us to investigate the influence of the choice of α on ϵ_1 and ϵ_2, the physical quantities of interest. The results obtained for example by fixing α to 0.65 and 0.70 for Au and Cu, respectively, are indicated in Figs. 3(a) and 4(a) (discontinuous curves).

In the differential experiments, we measured the quantity β for three angles of incidence $\theta = 50°$, $60°, 70°$. For the analysis of this data, R_{pure} for each value of θ was computed using for ϵ_1 and ϵ_2, the values determined previously and for α a value consistent with those determined from the pure metals experiments. R_{alloy} was then deduced from the experimental data and the same fitting procedure allowed to determine the complex dielectric constant of the alloy, α being fixed at the value chosen for the R_{pure} computation. Changing the values of α or its variation with energy in the whole procedure modified very little the shape and the magnitude of the $\Delta\epsilon_1$ and $\Delta\epsilon_2$ spectra, leaving the different structures at the same positions in energy.

B. Discussion of the results

Figure 5 shows the most reliable ϵ_1 and ϵ_2 spectra for pure Au between 18 and 34 eV (continuous curves). It must be recalled that, in the case of Au, the dependence on α is unfortunately quite critical and that the absolute values of ϵ_1 and ϵ_2 cannot be ascertained to better than ± 0.1 in most of this spectral range (except around 22 eV, where the accuracy is better). At high energies around 30 eV, the error is larger, ± 0.2. On the same figure, we have reported the spectra obtained by Hagemann et al.[25] by a Kramers-Krönig analysis performed on a set of available reflection or absorption data going from 10^{-3}–300 eV, some of them modified in order to match the

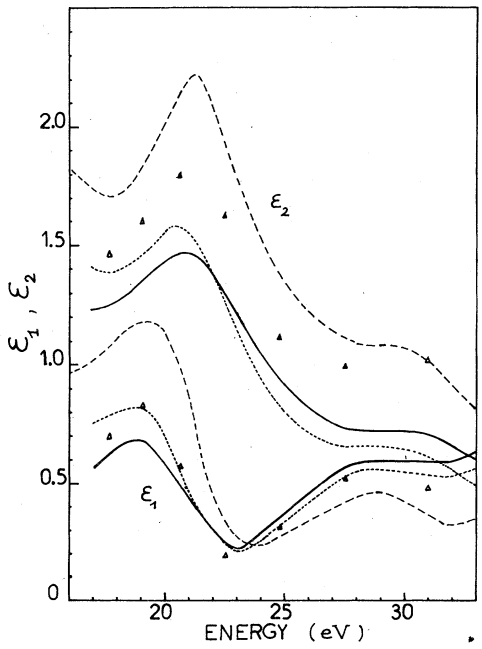

FIG. 5. ϵ_1 and ϵ_2 spectra between 18 and 34 eV for Au as deduced from the multiangle reflection data (continuous curves) and from the Kramers-Krönig analysis described in the text (dotted curves); the dashed curves represent the results given by Hagemann *et al.* (Ref. 25), the Δ represent the results obtained by Canfield *et al.* (Ref. 6).

other ones in the regions of overlap (discontinuous curves). These results correspond to the second version proposed by Hagemann *et al.*, which uses reflectivity data in the spectral range in which we are interested. Even in this case, there are important discrepancies, well beyond the limit of our errors, between these Kramers-Krönig results and our directly determined results. The general shape of the curves is nevertheless the same, and the gross features are located at the same energies. This illustrates the difficulties encountered when using a Kramers-Krönig analysis, even when data are available in a large energy range, if these data are not perfectly consistent (which is especially the case for Au, as pointed out by Hagemann *et al.*) and if the absolute values of the dielectric constant are not adjusted by fitting at one or more points to values ascertained by another method. On the same figure, we have also indicated some of the results obtained by Canfield *et al.*[6] by a multiangle reflection technique similar to ours, but with conventional sources. These values are in better agreement with ours, especially for ϵ_1; the values of ϵ_2 are greater in the whole spectral range, which must be related to the fact that the reflectivities which they measured were slightly higher than ours.

Figure 6 shows the ϵ_1 and ϵ_2 spectra, which we have obtained for pure Cu (continuous curves), together with the results of Hagemann *et al.*, deduced in a way similar to pure Au (discontinuous curves). In this case, the choice of α has much less importance in our method and these spectra are determined with an accuracy of ± 0.05 over most of the energy range; the uncertainty is only a little larger for ϵ_1 at high energies. One can see that here the agreement with the Kramers-Krönig curves is quite good both in shape and in absolute values; indeed the different data used for the Kramers-Krönig analysis were more reliable and consistent.

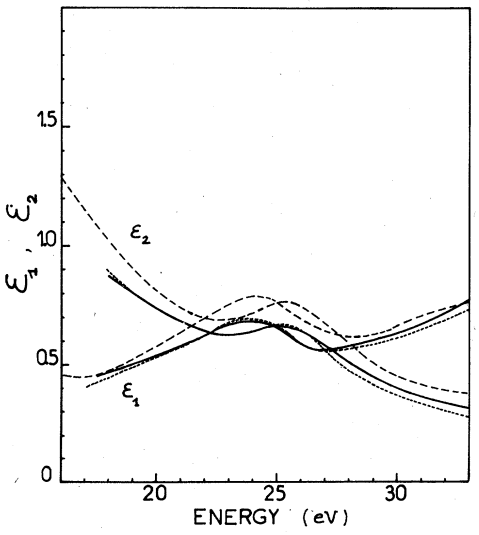

FIG. 6. ϵ_1 and ϵ_2 spectra between 18 and 34 eV for Cu as deduced from the multiangle reflection data (continuous curves) and from the Kramers-Krönig analysis described in the text (dotted curves); the dashed curves represent the results given by Hagemann *et al.* (Ref. 25).

In order to obtain the complex dielectric constant in a wider spectral range, and also to check the self-consistency of our results, we ourselves performed a Kramers-Krönig analysis of normal incidence reflectivity data chosen in the following way: for Au we took, between 18 and 34 eV, the R values computed from our most reliable ϵ_1 and ϵ_2 results (Fig. 5); between 2 and 6 eV, the R values computed from ϵ_1 and ϵ_2 determined by Thèye[26] from thin-film measurements; between 6 and 18 eV, the R values given by Canfield *et al.*[6] The Thèye and Canfield *et al.* results agree quite well at 6 eV, but it was necessary to progressively lower the latter above 12 eV to obtain a good match with our results at 18 eV. For energies lower than 2 eV, we used different Drude extrapolations, which only influenced the low-energy part of the final result. For energies greater than 34 eV, we used for R an extrapolation of the form $R(\omega) = R(\omega_{\max})(\omega_{\max}/\omega)^s$, where $\omega_{\max} = 34$ eV and s is an adjustable parameter.[27] s was determined by fitting the computed ϵ_1 and ϵ_2 at $\hbar\omega = 22$ eV to the values determined directly; we found $s = 3.25$. The same procedure was followed for Cu, using as reflectivity data, besides our R values between 18 and 33.5 eV, the values given by Canfield and Hass between 6 and 18 eV (Ref. 7) and the R values computed from ϵ_1 and ϵ_2 as determined by Johnson and Christy[28] between 0.65 and 6 eV from thin film measurements. In this case we found $s = 2.85$. The results obtained by our Kramers-Krönig analysis between 18 and 34 eV are shown in Figs. 5 and 6 (dotted lines). The agreement with the ϵ_1 and ϵ_2 curves determined directly from the reflectivity at different angles of incidence is very good for Cu, less good for Au, again because of the necessary scaling between the different sets of data in this case.

Figure 7 shows the optical conductivity $\hbar\omega\epsilon_2$ as a function of energy in the whole spectral range up to 34 eV for pure Au and pure Cu. These curves are in good agreement with those deduced from electron-energy-loss experiments.[29] The free-electron contribution at low energies, as well as the onset of interband transitions can be easily recognized. It is worth noting that for Cu,

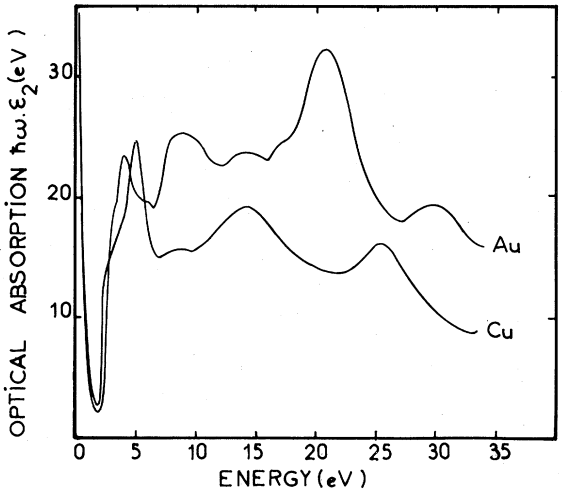

FIG. 7. Optical-absorption spectra $\hbar\omega\epsilon_2$ vs energy up to 34 eV as determined from the present data for Au and Cu.

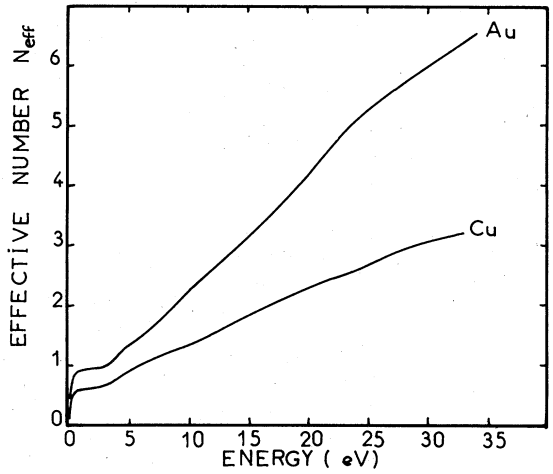

FIG. 8. Effective number of electrons N_{eff} as a function of energy computed from the results of Fig. 7 for Au and Cu.

the low-energy part of the interband conductivity, which is known to be essentially related to transitions from the whole d band (about 3 eV wide) to the conduction band at the Fermi level with some contribution of conduction band to conduction band transitions at L (critical point), is well separated from the two other main peaks, centered, respectively, at about 14.5 and 25.5 eV. The strength of the structures in the conductivity decreases as the energy increases. The spectrum for Au is remarkably more complicated, a striking feature being the high values of the conductivity at intermediate energies and the great concentration of oscillator strength around 21 eV.

Knowing ϵ_2 over such a large spectral range, we were able to compute the effective number of electrons involved in optical transitions as a function of energy, $N_{\text{eff}}(\omega)$, given by

$$\int_0^{\omega} \omega' \epsilon_2(\omega')\, d\omega' = \tfrac{1}{2}\pi\omega_p^2 N_{\text{eff}}(\omega)\,,$$

ω_p being the free-electron plasma frequency. Figure 8 shows these results. They are essentially similar to those obtained by Beaglehole,[8] only the absolute values are slightly different. One can see that N_{eff} rises very slowly with increasing energy for Cu, more rapidly for Au. A well-marked bump corresponds for Au to the large structure peaking at 21 eV in $\hbar\omega\epsilon_2(\omega)$. N_{eff} reaches 6.6 electrons per atom at 33 eV for Au, only 3.2 for Cu. The excitations of all available electrons: 1 for the conduction band and 10 for the d band, are far from being exhausted at this energy. Because of the lack of reliable experimental data at higher energies, we did not try to compute N_{eff} further.

We turn now to the investigation of the different structures which appear in the ϵ_1 and ϵ_2 spectra. For Au [Fig. 3(a)], ϵ_1 and ϵ_2 in the 18–25-eV range look very much like the complex dielectric constant for an oscillator, with a large peak between 18.5 and 22.5 eV in ϵ_2 and a characteristic maximum-minimum structure in ϵ_1. Some additional fine structure can be detected on the channeltron results which present lower noise: the main peak in ϵ_2 appears to be split, with two distinct maxima centered at about 20 and 21.4 eV. For Cu [Fig. 4(a)], ϵ_2 is much smaller than for Au in the low-energy range and it decreases slowly continuously with energy, except for a small bump centered at about 25 eV.

In order to investigate more precisely the fine structure which shows up in the ϵ_2 spectrum for Au, we have computed the derivative $\partial\epsilon_2/\partial\omega$. Figure 9 shows this spectrum in the 18–34-eV range, together with the derivative $\partial R/\partial\omega$ (deduced from the reflectivity curve at the angle of incidence 30°). It can be seen at once that $\partial R/\partial\omega$ presents more structure than $\partial\epsilon_2/\partial\omega$ and, moreover, that the structures in the two curves do not coincide. Indeed if the R and the ϵ_2 spectra both display the same overall shape with a large peak at low energies and a bump superimposed on the decrease at higher energies, the main peak, while starting at about the same energy, is centered at much lower energy in ϵ_2 (about 21 eV) than in R (about 22.5 eV). This shift comes from the fact that the spectral dependence of ϵ_1 also influences the R shape. The ϵ_2 derivative spectrum confirms that the ϵ_2 peak indeed presents two maxima separated by about 1.5 eV. At higher

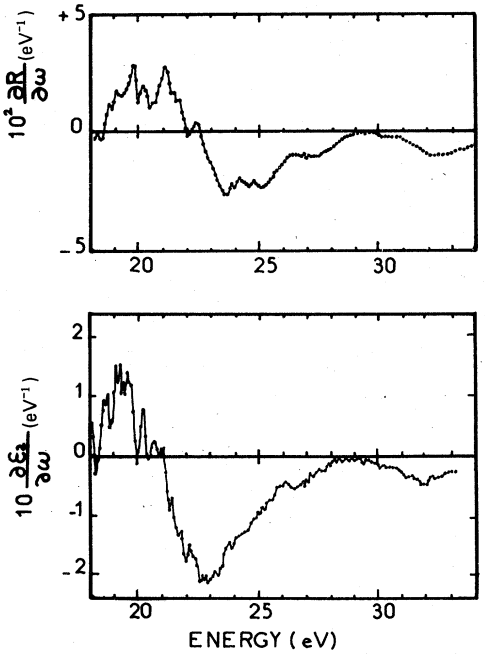

FIG. 9. Derivative spectra $\partial R/\partial\omega$ and $\partial\epsilon_2/\partial\omega$ between 18 and 34 eV for Au.

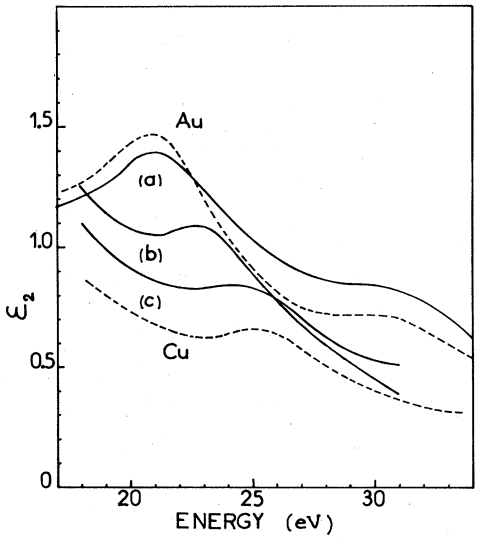

FIG. 10. ϵ_2 spectra between 18 and 30 or 34 eV for three AuCu alloys with Cu concentration equal to (a) 10.5, (b) 68 and (c) 92 at.%; the spectra of pure Au and pure Cu are also indicated.

energies, $\partial\epsilon_2/\partial\omega$ shows little structure except around 30 eV, while $\partial R/\partial\omega$ shows secondary structure in R around 24.5 and 26.5 eV. It is worth noting that the analysis of thermoreflectance measurements on Au in this spectral range also showed that the $\Delta\epsilon_2$ spectrum presented less fine structure than the ΔR spectrum.[13] Clearly measurements of R alone are not enough to discuss characteristics of optical absorption, at least for these metals. Determination of the behavior of the complex dielectric constant is absolutely necessary.

We have determined by the same methods the complex dielectric constant of several Au-Cu alloys deposited by coevaporation of the two metals and annealed in situ. Figure 10 shows the ϵ_2 spectra for three alloys with Cu concentrations equal to (a) 10.5, (b) 68, and (c) 92 at.%, respectively, as well as for pure Au and pure Cu. On the Cu-rich side, the comments already made for pure Cu on the determination of ϵ_2 also apply to the alloys; curves (b) and (c) are therefore determined with good accuracy. The overall shape of both ϵ_1 and ϵ_2 curves remains very much Cu-like, even for a Au concentration as large as 32%. The only effects of alloying on ϵ_2 are to shift the characteristic bump to lower energies (to 24–24.5 eV and 22.5–23 eV, respectively), to make it more pronounced, and to enhance the values in the low-energy range.

On the Au-rich side, the same difficulties as for pure Au were encountered in the determination of the dielectric constant; the absolute values in curve (a) must therefore be considered as approximate (they are moreover deduced from channeltron data). However, this curve is practically identical in its shape to the pure Au one. In order to confirm this observation, we have computed both $\partial R/\partial\omega$ and $\partial\epsilon_2/\partial\omega$ for the alloy; no significant differences with the derivatives for pure Au can be detected, except perhaps in the details of fine structure of the main ϵ_2 peak.

In order to understand what happens at intermediate Cu concentrations, we have studied an alloy with 32 at.% of Cu, this time by the differential method. Figure 11 shows the $\Delta\epsilon_1$ and $\Delta\epsilon_2$ spectra deduced from these measurements. Both present essentially a large peak, positive for $\Delta\epsilon_1$, negative for $\Delta\epsilon_2$, in the region of the main peak in ϵ_2 for pure Au, with a subsidiary small wing of opposite sign at lower energy. A two-minima structure can be detected in the main peak of $\Delta\epsilon_2$, corresponding roughly to the fine structure in ϵ_2 for pure Au. The effects of alloying in this particular case seem therefore to be a broadening of the absorption edge of pure Au and an appreciable reduction of the characteristic peak in the 20–24-eV range. This would lead for the alloy to ϵ_1 and ϵ_2 curves looking more Cu-like than Au-like, with a bump centered at about 19.5–20 eV superimposed on a large background decreasing with increasing energy.

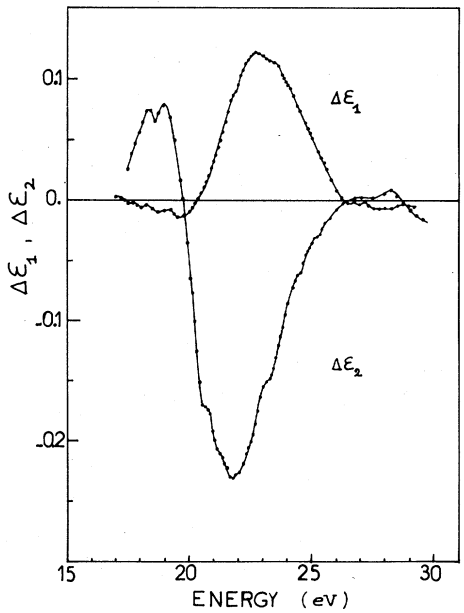

FIG. 11. Variations of the complex dielectric constant of Au upon alloying with Cu: $\Delta\epsilon_1$ and $\Delta\epsilon_2$ as a function of energy for a Cu concentration of 32 at.%, as determined from the differential reflectivity data with $\alpha = 0.64$.

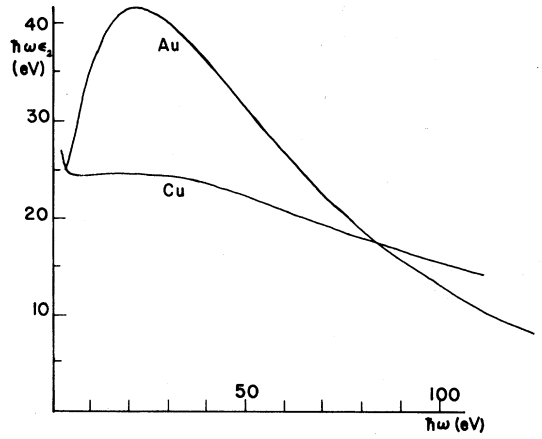

FIG. 12. Optical conductivity $\hbar\omega\epsilon_2$ for Cu and Au calculated using the model of atomic d states excited to plane-wave final states.

IV. CONCLUSION

As we have already noted, the overall absorption of Au is seen in Fig. 7 to be stronger than that of Cu. The simple model outlined by Beaglehole[15] which estimated the absorption by atomic d electrons excited to free-electron final states indicates just this enhanced absorption. Figure 12 shows the absorption spectrum calculated with this model using Herman and Skillman's[30] atomic d wave functions. The enhanced absorption is due to the more spatially extended Au 5d states in comparison with the Cu 3d states.

While band structure calculations have been carried through for Cu (Refs. 9, 31) and Au,[10,11] which can provide some indication of the energies of critical structures, there are unfortunately no calculations of the optical absorption in our energy range to compare with experiment. Since the d bands are quite flat, the dominant features are likely to be associated with the conduction band, and the peaks will be associated with large regions of k space in which the conduction bands are reasonably flat and where the matrix elements favor excitation. Hermanson *et al.*[14] have assigned the dominant Au peak at 21 eV to excitations at the center of the Brillouin zone (Γ). To us this seems unlikely, since estimates show that the structure in the density of final states around Γ is weak. It appears much more likely that the structure will be associated with states near the edge of the Brillouin zone. The doublet seen in our results in the Au peak (splitting 1.5 eV) indicates that two critical points are involved, either from d-band structure or associated with two final states. This splitting of the Au peak has also been observed in thermoreflectance measurements made by Olson et al.,[12] who report features at 19.8 and 21.0 eV. Piacentini[13] comments that a line-shape analysis of the thermoreflectance $\Delta\epsilon$ clearly indicates that these transitions do not occur at Γ, which is in agreement with our own conclusions.

Janak *et al.*[2] have found that they were able to obtain a good comparison between photoemission experiments and theory for Cu for photon energies up to 25 eV by applying a "self-energy" correction to the band energies, which involved a stretching of the band states above the Fermi level by about 8%. Without this stretching, final states at Γ lie in range to produce the observed optical peaks, but with this stretching, and assuming a similar stretching to occur also for Au excitations, states at X and K of the Brillouin zone fall in the appropriate range for this optical structure. Recent angular-resolved photoemission experiments on Cu (Refs. 32, 33, 34) have confirmed the conclusions of Janak *et al.*, and have been able to map out sections of the Cu d band. The last authors[34] have noted that Au appears to show unusual final states; we will return to this below.

We turn to the alloy data, and here we find a somewhat unusual behavior. We would expect the two related peaks to move continuously from the energy of one pure metal to the other on alloying. In fact this only occurs on the Cu-rich side; the

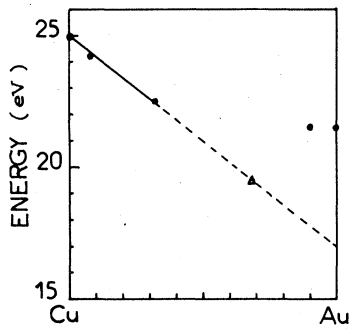

FIG. 13. Variation of the position in energy of the peak in ϵ_2 with Au concentration for Cu-Cu alloys: (●) static measurements on alloys; (Δ) estimated from differential measurements.

peak energies are plotted versus alloy concentration in Fig. 13, the rate of variation of the excitation energy being −0.08 eV/at.%. On the Au-rich side we observe no shift, only a reduction in strength.

Low-energy optical studies of these alloys[20,35] measuring the onset of *d* to Fermi-level excitations have shown that the *d* states move continuously from the energy of one pure metal to the other on alloying. The data of Beaglehole and Erlbach can be analyzed to show that the top of the *d* band moves upwards with respect to the bottom of the conduction band from Au to Cu, almost linearly. (We obtain a shift rate of 0.02 eV/at.% on the Au-rich side and 0.03 eV/at.% on the Cu-rich side.) Thus the implications of our alloy data must be that the final-state critical points move on the Cu-rich side downwards at a rate of about −0.05 eV/at.% and on the Au-rich side upwards at a rate of about +0.02 eV/at.%.

This sort of asymmetry in the motion of band states is not unreasonable. Indeed a parabolic behavior of critical points is the usual observation even at low-excitation energies.[20,35,36] At high-excitation energies one might expect even stronger asymmetries than at low-excitation energies, since the Au atomic potential has low-lying empty 5*f* states which are absent in the case of Cu. Several authors have commented that these empty low-lying 5*f* states in the Au atomic potential may be an important factor in the optical absorption of Au.[12,17] If they are present, then an alternative explanation for the alloy results is possible. The 5*f* states appearing only in the Au potential would lead to localized excitations around the Au atoms, and so their associated structure would not move on alloying with Cu.

ACKNOWLEDGMENTS

The authors are very indebted to Dr. B. Thiéblemont for his participation in the experimental part of this work, to D. Pailharey for his help with the equipment, and to the members of the Laboratorie de l'Accélérateur Linéaire (Orsay) for their assistance with operating the ACO storage ring. We would also like to thank Professor J. Hanus for his active support and valuable comments, and Professor F. Abelès for his constant interest. Partial financial support from the Délégation Gènèrale à la Recherche Scientifique et Technique under Contract No. 73-7-1583 is gratefully acknowledged.

*Present address: Physics Dept., Victoria Univ. of Wellington, Wellington, New Zealand.
†Present address: Laboratoire d'Optique des Solides, Université P. et M. Curie, Paris, France.

[1]For a review, see P. O. Nilsson, in *Solid State Physics*, edited by H. Ehrenreich, F. Seitz, and D. Turnbull (Academic, New York, 1974), Vol. 29, p. 139.
[2]A. R. Williams, J. F. Janak, and V. L. Moruzzi, Phys. Rev. Lett. 28, 671 (1972); J. F. Janak, A. R. Williams, and V. L. Moruzzi, Phys. Rev. B 11, 1522 (1975).
[3]W. G. Walker, O. P. Rustgi, and G. L. Weissler, J. Opt. Soc. Am. 49, 471 (1959).
[4]H. Ehrenreich and H. R. Philipp, Phys. Rev. 128, 1622 (1962).
[5]B. R. Cooper, H. Ehrenreich, and H. R. Philipp, Phys. Rev. 138, 1494 (1965).
[6]L. R. Canfield, A. Hass, and W. R. Hunter, J. Phys. (Paris) 25, 124 (1964).
[7]L. R. Canfield and G. Hass, J. Opt. Soc. Am. 55, 61 (1965).
[8]D. Beaglehole in *Optical Properties and Electronic Structure of Metals and Alloys*, edited by F. Abelès (North-Holland, Amsterdam, 1966), p. 154; Proc. Phys. Soc. London 87, 461 (1966).
[9]G. A. Burdick, Phys. Rev. 129, 138 (1963).
[10]J. W. D. Connolly and K. H. Johnson, Massachusetts Institute of Technology Solid State and Molecular Theory Group Report No. 72, 1970 (unpublished), p. 19.
[11]N. E. Christensen, Phys. Rev. B 13, 2698 (1976).
[12]C. G. Olson, M. Piacentini, and D. W. Lynch, Phys. Rev. Lett. 33, 644 (1974).
[13]M. Piacentini, Nuovo Cimento B 39, 682 (1977).
[14]J. Hermanson, J. Anderson, and G. Lapeyre, Phys. Rev. B 12, 5410 (1975).
[15]D. Beaglehole, Proc. Phys. Soc. London 85, 1007 (1965).
[16]J. Thomas, J. C. Lemonnier, and S. Robin, Opt. Acta 19, 983 (1972).
[17]D. Beaglehole and B. Thiéblemont, Nuovo Cimento B 39, 477 (1977).
[18]J. D. E. McIntyre in *Advances in Electrochemistry and Electrochemical Engineering*, edited by R. M. Muller (Wiley, New York, 1973), Vol. 9, p. 61.
[19]D. Beaglehole, M. de Crescenzi, B. Thiéblemont, Nguyen Binh, M. L. Thèye, and G. Vuye, *Extended Abstracts of the Fifth International Conference on*

Vacuum Ultra Violet (CNRS, Meudon, 1977), Vol. II, p. 74.
[20]D. Beaglehole and E. Erlbach, Phys. Rev. B 6, 1209 (1972).
[21]B. O. Seraphin in *Optical Properties of Solids*, edited by F. Abelès (North-Holland, Amsterdam, 1972), p. 163.
[22]G. Jezequel, J. Thomas, and J. C. Lemonnier (private communication).
[23]P. R. Bevington, *Data Reduction and Error Analysis for the Physical Sciences* (McGraw-Hill, New York, 1969).
[24]Technical Notice of the Fortran Program BMDX-85 from the Health Sciences Computing Facility, UCLA (unpublished); and R. I. Jennrich and P. F. Sampson, Technometrics 10, 63 (1968).
[25]H. J. Hagemann, W. Gudat, and C. Kunz, DESY SR 74/7, 1974 (unpublished).
[26]M.L. Thèye, Phys. Rev. B2, 3060 (1970).
[27]For example, see D. L. Greenaway and G. Harbeke, *Optical Properties and Band Structure of Semiconductors* (Pergamon, London, 1968).
[28]P. B. Johnson and R. W. Christy, Phys. Rev. B 6, 4370 (1972).
[29]C. Wehenkel, J. Phys. 36, 199 (1975).
[30]F. Herman and S. Skillman, *Atomic Structure Calculations* (Prentice Hall, New York, 1963).
[31]B. Segall, Phys. Rev. 125, 109 (1962).
[32]D. Leibowitz, M. Sagurton, J. Colbert, and N. J. Shevchik, Phys. Rev. Lett. 39, 1625 (1977).
[33]J. Stohv, P. S. Wehner, R. S. Williams, and D. A. Shirley, Phys. Rev. B 17, 587 (1978).
[34]S. P. Weeks and J. E. Rowe, Bull. Am. Phys. Soc. 23, 207 (1978).
[35]J. Rivory, Phys. Rev. B 15, 3119 (1977).
[36]E. A. Stern, Phys. Rev. 144, 545 (1966).

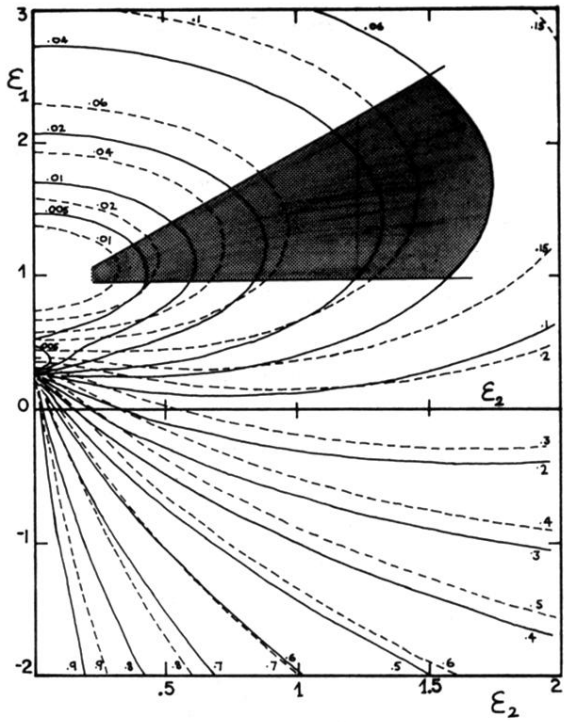

FIG. 1. Isoreflectance curves in the (ϵ_1, ϵ_2) plane for the two extreme values of the polarization α: 0.0 (continuous lines) and 1.0 (dashed lines), and for the angle of incidence $\theta = 30°$. The shaded area indicates the region of sensitivity to ϵ_2.